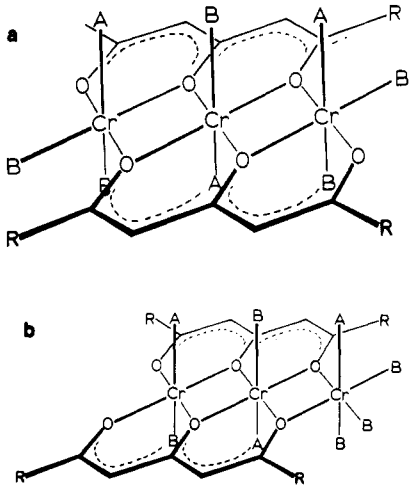

Figure 2. Probable structures for the linear trinuclear complex: (a) symmetrical structure, considered more likely; (b) unsymmetrical structure (A = H_2O, B = OH^-, R = phenyl).

$= x^5(y^{12} + x^6y^6 + x^{10}y^2)$, $A_4 = 2(y^{12} + x^6y^6 + x^{10}y^2 + x^{12})$, $A_5 = x^3y^2(y^4 + x^4)$, $x = e^{2J/kT}$, $y = e^{2J'/kT}$, and the other terms have their usual meaning.

To eliminate g as a fitting parameter, the ESR g value of 1.977 was used, and temperature-independent paramagnetism was taken as zero. Pure antiferromagnetism is observed with $|J| > |J'|$. The best fit is with $J = -6.00$ cm^{-1} and $J' = -1.35$ cm^{-1} with $\delta' = 8.46 \times 10^{-7}$. The g value from the Curie–Weiss and ESR calculations is supported by the observation that the agreement between eq 2 and the observed values becomes worse if the g value is varied significantly from 1.977. Increasing the number of fitting parameters over the two used here necessarily improves the agreement. Thus, with a 3% paramagnetic impurity, a slightly better fit is calculated with $J = -7.35$ cm^{-1} and $J' = -4.06$ cm^{-1}. However, the effect of paramagnetic impurity is likely to be overestimated if other small effects on the magnetism are omitted. These include biquadratic exchange and interactions between adjacent molecules, as well as experimental error. Though none of these would be large, their effects on the magnetism are not independent and not easily evaluated; in the absence of crystallographic data, the intermolecular distance is unknown, but the relatively bulky nature of the ligands should keep intermolecular interaction from being very important.

Table II. UV-Visible Band Positions (cm^{-1}) for $Cr(C_{17}H_{12}O_3)_2(H_2O)_3(OH)_5$ and $Cr(DBM)_3$

trimer (MeOH)	monomer ($CHCl_3$)	assignment[16]
19230	17480	$^4A_{2g} \rightarrow {}^4T_{2g}$
23877	21080	L → M
30057	25810	L → M
39682	32470	$\pi \rightarrow \pi^*$

A decidedly poorer fit is obtained for an equilateral triangle model. The only way to get a fit at all is to assume a paramagnetic impurity. However, an improbably large impurity must be assumed: the best fit in this case is obtained when the impurity is 9% and $J = J' = -14.65$ cm^{-1}; the deviation factor is still doubled ($\delta' = 1.92 \times 10^{-6}$). Therefore, ruling out the equilateral triangular arrangement, we propose a linear trinuclear structure as shown in Figure 2. The linear arrangement can be realized with the two extreme metal atoms identical in the symmetrical structure (Figure 2a). The magnetic model is based on this type of geometry. The unsymmetrical linear structure (Figure 2b) would have three unique metal sites. These three sites may not be sufficiently different to be distinguishable, so that the unsymmetrical structure cannot be ruled out. We have not been able to obtain crystals suitable for X-ray crystallographic study. However, since the ligand remains rigidly planar in all dimeric systems, it is reasonable to assume planarity here also with edge–edge-bound octahedra.

The UV-visible spectral data for the trinuclear complex and for the corresponding mononuclear β-diketonate, $Cr(DBM)_3$,[23] are given in Table II. This also supports the proposed structure. As the spectrum is typical of octahedral Cr(III), the triketonate ligands appear to be coordinated and bridging in the customary manner. This requires a planar molecule with the three Cr(III) species in a linear or very shallow isosceles triangular arrangement. All peaks are shifted to higher energy in the trinuclear complex, as might be expected, attesting to the coupling of the metal atoms in this complex.

Acknowledgment. Support under a CSUS Faculty Research Grant and NSF Grants CHE83-00516 and CHE83-11449 is gratefully acknowledged.

(23) Fatta, A. M.; Lintvedt, R. L. *Inorg. Chem.* **1971**, *10*, 478.

Contribution from the Department of Chemistry and Laboratory for Molecular Structure and Bonding, Texas A&M University, College Station, Texas 77843, and Department of Chemistry, The Technion-Israel Institute of Technology, Haifa, Israel

Oxidative Fragmentation of the Cuboid Mo_4S_4 Cluster Core: Synthesis and Structures of $[Mo_3(\mu_3\text{-}S)(\mu\text{-}S)_3([9]aneN_3)_3]^{4+}$ and $\{[MoO([9]aneN_3)]_2(\mu\text{-}S)_2\}^{2+}$

F. Albert Cotton,*† Zvi Dori,*‡ Rosa Llusar,† and Willi Schwotzer†

Received April 9, 1986

The reaction of the cuboid $[Mo_4S_4]^{6+}$ aquo ion with the terdentate cyclic amine 1,4,7-triazacyclononane ([9]aneN$_3$) initially yields a brown solution from which, depending on the reaction conditions, two fragmentation products were isolated. In acidic solution (pH <2) a trinuclear cluster, $[Mo_3(\mu_3\text{-}S)(\mu\text{-}S)_3([9]aneN_3)_3](ZnCl_4)(ZnCl_3OH_2)_2\cdot 3H_2O$, was isolated. It crystallizes in the orthorhombic space group $Pn2_1a$ with $a = 14.116$ (3) Å, $b = 16.417$ (6) Å, $c = 20.773$ (9) Å, $V = 4814$ (5) Å^3, and $Z = 4$. The cluster cation belongs to the M_3X_{13} type (incomplete cube). In neutral medium (pH ≈7) a dinuclear bis(thio)-bridged compound of oxomolybdenum(V) is isolated, $\{[MoO([9]aneN_3)]_2(\mu\text{-}S)_2\}(PF_6)_2$. It crystallizes in the monoclinic space group $P2_1/c$ with $a = 7.124$ (2) Å, $b = 12.158$ (2) Å, $c = 16.241$ (5) Å, $\beta = 90.88$ (2)°, $V = 1406$ (1) Å^3, and $Z = 4$. The dimeric unit consists of two octahedrally coordinated Mo atoms sharing an edge. The oxo ligands are in an anti configuration with respect to the $Mo(\mu\text{-}S)_2Mo$ plane.

Introduction

It has become apparent recently that an important aspect of the aqueous chemistry of the early transition metals is the presence of polynuclear species, in many of which there are metal–metal bonds.[1,2] The cores of these clusters often are robust entities that can be isolated, in aquated form, by ion-exchange chromatography.

† Texas A&M University.
‡ The Technion-Israel Institute of Technology.

(1) Cotton, F. A.; Wilkinson, G. *Advanced Inorganic Chemistry*, 4th ed.; Wiley: New York, 1980; pp 867–872.
(2) Richens, D. T.; Sykes, A. G. *Comments Inorg. Chem.* **1981**, *1*, 151.

0020-1669/86/1325-3654$01.50/0

Table I. Crystal Data for Compounds **2** and **3**

	2	**3**
formula	$[Mo_3S_4(N_3C_6H_{15})_3][ZnCl_4][ZnCl_3(H_2O)]_2 \cdot 3H_2O$	$[Mo_2S_2O_2(N_3C_6H_{15})_2](PF_6)_2$
fw	1444.4	836.35
space group	$Pn2_1a$	$P2_1/c$
syst absences	$(0kl)$, $h + l = 2n + 1$; $(hk0)$, $h = 2n + 1$; $(h00)$, $h = 2n + 1$; $(0k0)$, $k = 2n + 1$; $(00l)$, $l = 2n + 1$	$(h0l)$, $l = 2n + 1$; $(0k0)$, $k = 2n + 1$
a, Å	14.116 (3)	7.124 (2)
b, Å	16.417 (6)	12.158 (2)
c, Å	20.773 (9)	16.241 (1)
β, deg		90.88 (2)
V, Å^3	4814 (5)	1406 (1)
Z	4	2
d_{calcd}, g/cm^3	1.99	1.975
cryst size, mm	0.2 × 0.1 × 0.15	0.2 × 0.1 × 0.05
μ(Mo Kα), cm^{-1}	30.17	12.27
data collcn instrum	Enraf-Nonius CAD-4	
radiation monochromated in incident beam (λ_α,Å)	Mo Kα (0.71073)	
orientation reflcns: no.; range (2θ), deg	25; 15–27	25; 20–30
temp, °C	25	25
scan method	ω	ω–2θ
data collcn range (2θ), deg	4–42; $+h,+k,+l$ to $-h,-k,-l$	4–45
no. of unique data, total with $F_o^2 > 3\sigma(F_o^2)$	3990, 2569	1830, 1034
no. of params refined	308	142
R,[a] %	4.94	5.8
R_w,[b] %	5.73	7.07
quality-of-fit indicator[c]	1.256	1.8
largest shift/esd, final cycle	0.01	0.01
largest peak, e/Å^3	1.224	0.68

[a] $R = \sum||F_o| - |F_c||/\sum|F_o|$. [b] $R_w = [\sum w(|F_o| - |F_c|)^2/\sum w|F_o|^2]^{1/2}$; $w = 1/\sigma^2(|F_o|)$. [c] Quality-of-fit = $[\sum w(|F_o| - |F_c|)^2/(N_{observns} - N_{params})]^{1/2}$.

Although these polynuclear aquo ions themselves are notoriously difficult to crystallize, many of their derivatives have been structurally characterized.

Recently the cuboidal cluster aquo ion $[Mo_4S_4]_{aquo}$ has been prepared by Sykes[3] as well as by us[4] employing different synthetic routes, and we have determined the structure of a thiocyanato derivative, $[Mo_4S_4(NCS)_{12}]^{6-}$ (**1**). Calculations made in an attempt to rationalize the chemical bonding, in particular the observed Jahn–Teller distortion, indicated that there is a substantial contribution of the SCN sulfur orbitals to the orbitals that pertain to the bonding within the cluster core. In order to minimize this ligand contribution and thus to model more closely the situation in the aquo species, we reacted the latter with 1,4,7-triazacyclononane ([9]aneN$_3$), a cyclic triamine that is tailor-made for occupying three *fac* sites in octahedral coordination polyhedra.

We report here the molecular structures of two compounds, $[Mo_3(\mu_3\text{-}S)(\mu\text{-}S)_3([9]aneN_3)_3]^{4+}$ (**2**) and $\{[MoO([9]aneN_3)]_2(\mu\text{-}S)_2\}^{2+}$ (**3**), which are obtained from **1** and [9]aneN$_3$ after workup in acidic and neutral conditions, respectively.

Experimental Section

The ligand 1,4,7-triazacyclononane in the form of the trihydrobromide was a generous gift from Professor Karl Wieghardt. The free amine was prepared according to his procedure.[5]

The $[Mo_4S_4]$ aquo ion was prepared, purified and freeze-dried as previously described.[6] An aqueous solution was obtained by dissolving the green powder in degassed H_2O. The concentration of the resulting solution is conveniently determined by UV absorption.

Preparation of $[Mo_3(\mu_3\text{-}S)(\mu\text{-}S)_3([9]aneN_3)_3](ZnCl_4)(ZnCl_3OH_2)\cdot 3H_2O$ (2) and $\{[MoO([9]aneN_3)]_2(\mu\text{-}S)_2\}(PF_6)_2$ (3). To a ca. 4×10^{-3} M solution of **1** in degassed H_2O a 3 molar excess of the solid amine was added under a blanket of argon. The color of the solution changed from green to brown, and the previously clear solution turned slightly turbid. Stirring was continued under argon for 24 h before the solution was filtered.

At this point the preparations of **2** and **3** diverged. To one fraction of the solution was added solid $ZnCl_2$ (4 molar excess) and the pH of the solution adjusted to pH 2 with HCl (concentrated) in order to foster the formation of the $ZnCl_4^{2-}$ anion, which is, in our experience, an excellent counterion for the crystallization of cluster cations. The beaker containing the acidic solution was covered with perforated paraffin film and set in air for slow crystallization. A change of color from brown to green was observed after 24 h, and the blue-green crystals of **2** deposited within 1 week. Yield (M_3 from M_4): ca. 60%.

To another portion of the reaction mixture was added solid NH_4PF_6 (5 molar excess) to yield an initially brown solution of neutral pH. Orange crystals of **3** deposited in ca. 50% yield in 3 days of slow evaporation.

X-ray Crystallography

(a) $[Mo_3(\mu_3\text{-}S)(\mu\text{-}S)_3([9]aneN_3)_3](ZnCl_4)(ZnCl_3OH_2)_2\cdot 3H_2O$ (2). A blue-green crystal of dimensions 0.20 × 0.10 × 0.15 mm was mounted on the end of a thin glass fiber with epoxy glue. Twenty-five reflections in the range $15° \le 2\theta \le 27°$ were located by using the automatic search routine on an Enraf-Nonius CAD-4 diffractometer. The automatic indexing routine followed by least-squares analysis produced the unit cell parameters. Table I summarizes the data pertaining to the crystallographic procedures and refinement.[7] During data collection three intensity standards were collected every 100 reflections. No decay was observed during the 71.1 h of exposure to X-rays. Lorentz and polarization corrections were applied to the measured intensities.

Data were collected according to the orthorhombic crystal system. The systematic absences ($(0kl)$, $k + l = 2n + 1$; $(hk0)$, $h = 2n + 1$; $(h00)$, $h = 2n + 1$); $(0k0)$, $k = 2n + 1$; $(00l)$, $l = 2n + 1$) limited the possible space groups to *Pnma* or $Pn2_1a$. The unit cell volume was suggestive for $Z = 4$. In *Pnma* this requires the trinuclear unit to be located on a special position of which only the mirror plane concurs with the molecular symmetry. After the Patterson map showed a metal–metal vector parallel to the mirror plane, it was clear that the trinuclear unit could not be accommodated in an ordered model in *Pnma*. The structure was therefore developed in the noncentrosymmetric space group $Pn2_1a$. Since the amount of data was limited by the small size and moderate diffraction quality of the crystals, Friedel pairs (which are independent observations in a noncentrosymmetric space group) were collected in order to improve the data:parameter ratio.

The structure developed smoothly. The final difference Fourier map indicated a small degree of disorder at the $ZnCl_3(H_2O)$ sites, but no effort was made to refine alternative orientations. In order to maintain

(3) Kathirgamanthan, P.; Martinez, M.; Sykes, A. G. *J. Chem. Soc., Chem. Commun.* **1985**, 953.
(4) Cotton, F. A.; Diebold, M. P.; Dori, Z.; Llusar, R.; Schwotzer, W. *J. Am. Chem. Soc.* **1985**, *107*, 6735.
(5) Wieghardt, K.; Schmidt, W.; Nuber, D.; Weiss, J. *Chem. Ber.* **1979**, *112*, 2228.
(6) Cotton, F. A.; Dori, Z.; Llusar, R.; Schwotzer, W., submitted for publication in *Inorg. Chem.*

(7) The Enraf-Nonius Structure Determination Package (VAXSDP) was used for all crystallographic computation on a VAX-11/780 computer.

Table II. Positional Parameters and Their Estimated Standard Deviations for Compound **2**

atom	*x*	*y*	*z*	*B*, Å^2
Mo(1)	0.5032 (1)	0.5125 (2)	0.42942 (9)	2.42 (4)
Mo(2)	0.3429 (1)	0.541	0.5025 (1)	2.38 (4)
Mo(3)	0.5148 (1)	0.5117 (1)	0.56297 (9)	2.43 (4)
Zn(1)	0.2482 (2)	0.7692 (2)	0.1995 (1)	4.41 (7)
Zn(2)	0.2200 (2)	0.2603 (2)	0.3233 (1)	3.92 (7)
Zn(3)	0.4068 (2)	0.3761 (2)	0.0235 (2)	4.72 (8)
Cl(11)	0.2485 (5)	0.9063 (4)	0.2120 (3)	4.5 (2)
Cl(12)	0.1620 (6)	0.7447 (5)	0.1127 (3)	5.8 (2)
Cl(13)	0.206 (1)	0.7083 (6)	0.2869 (5)	12.5 (4)
Cl(21)	0.3253 (6)	0.2454 (5)	0.4013 (4)	6.0 (2)
Cl(22)	0.2184 (5)	0.3963 (4)	0.3041 (3)	4.5 (2)
Cl(23)	0.2280 (6)	0.1856 (5)	0.2349 (3)	5.5 (2)
Cl(31)	0.2584 (4)	0.3207 (4)	0.0147 (3)	4.1 (2)
Cl(32)	0.4410 (6)	0.4147 (6)	0.1230 (4)	8.1 (3)
Cl(33)	0.5063 (6)	0.2743 (5)	−0.0024 (5)	9.0 (2)
Cl(34)	0.4191 (6)	0.4849 (6)	−0.0394 (5)	10.1 (3)
S(1)	0.4288 (4)	0.4184 (3)	0.4984 (3)	2.6 (1)
S(2)	0.3984 (4)	0.6172 (4)	0.4186 (3)	2.6 (1)
S(3)	0.4127 (5)	0.6168 (4)	0.5822 (3)	3.4 (2)
S(4)	0.6113 (4)	0.5767 (4)	0.4925 (3)	3.3 (1)
O(1)	0.386 (2)	0.736 (2)	0.187 (1)	11.6 (8)*
O(2)	0.100 (1)	0.224 (1)	0.3641 (9)	6.5 (5)*
O(3)	0.970 (2)	0.335 (2)	0.664 (1)	10.9 (7)*
O(4)	0.426 (2)	0.255 (2)	0.195 (1)	12.0 (8)*
O(5)	0.405 (3)	0.614 (2)	0.092 (2)	17 (1)*
N(10)	0.608 (1)	0.417 (1)	0.4022 (9)	3.4 (5)*
N(11)	0.579 (1)	0.569 (1)	0.3464 (9)	3.4 (5)*
N(12)	0.434 (1)	0.447 (1)	0.3395 (9)	3.5 (5)*
N(20)	0.236 (1)	0.481 (1)	0.5701 (8)	2.5 (4)*
N(21)	0.227 (1)	0.484 (1)	0.4404 (8)	2.9 (4)*
N(22)	0.222 (1)	0.627 (1)	0.5069 (9)	3.1 (4)*
N(30)	0.605 (1)	0.566 (1)	0.6411 (8)	2.2 (4)*
N(31)	0.625 (1)	0.413 (1)	0.5844 (9)	3.5 (5)*
N(32)	0.467 (1)	0.445 (1)	0.6551 (8)	2.5 (4)*
C(10)	0.562 (2)	0.347 (2)	0.371 (1)	4.1 (6)*
C(11)	0.495 (2)	0.373 (2)	0.321 (1)	5.1 (7)*
C(12)	0.441 (2)	0.513 (2)	0.288 (1)	3.9 (5)*
C(13)	0.537 (2)	0.546 (2)	0.281 (1)	4.5 (6)*
C(14)	0.680 (2)	0.532 (2)	0.346 (1)	4.0 (6)*
C(15)	0.684 (2)	0.441 (2)	0.356 (1)	4.3 (7)*
C(20)	0.159 (2)	0.546 (2)	0.414 (1)	5.6 (7)*
C(21)	0.145 (2)	0.616 (1)	0.453 (1)	3.0 (5)*
C(22)	0.165 (2)	0.622 (2)	0.568 (1)	5.4 (7)*
C(23)	0.169 (2)	0.542 (2)	0.598 (1)	5.8 (7)*
C(24)	0.189 (2)	0.413 (1)	0.545 (1)	3.9 (6)*
C(25)	0.174 (2)	0.420 (2)	0.476 (1)	4.2 (7)*
C(30)	0.701 (2)	0.535 (2)	0.630 (1)	4.6 (6)*
C(31)	0.706 (2)	0.441 (2)	0.626 (1)	3.6 (6)*
C(32)	0.573 (2)	0.338 (1)	0.613 (1)	3.4 (5)*
C(33)	0.523 (2)	0.369 (1)	0.672 (1)	3.8 (6)*
C(34)	0.475 (2)	0.509 (2)	0.709 (1)	4.8 (6)*
C(35)	0.572 (2)	0.550 (1)	0.708 (1)	3.4 (5)*

[a] Values marked with an asterisk indicates that the atoms were refined isotropically. Anisotropically refined atoms are given in the form of the isotropic equivalent thermal parameter defined as $^4/_3[a^2\beta_{11} + b^2\beta_{22} + c^2\beta_{33} + ab(\cos\gamma)\beta_{12} + ac(\cos\beta)\beta_{13} + bc(\cos\alpha)\beta_{23}]$.

a reasonably high parameter-to-data ratio, all oxygen, nitrogen, and carbon atoms were refined isotropically. The last least-squares cycle yielded agreement factors of $R = 0.0494$ and $R_w = 0.0573$ for the fit of 308 variables to 2569 data with $F_o^2 \geq 3\sigma(F_o^2)$. The value of R for the alternative enantiomer was 0.053.

(b) {[MoO([9]aneN$_3$)]$_2$(μ-S)$_2$}(PF$_6$)$_2$ (3). The crystals of **3** grew as clusters of three-dimensional stars. Inspection under polarized light indicated that the individual points were singly crystalline. Several of these fragments were gently chipped off and surveyed on an automated four-circle diffractometer. The unit cell dimensions were established by automated routines and, together with the Laue class, confirmed by axial photography. The monoclinic space group $P2_1/c$ was uniquely determined by the systematic absences.

The position of the unique Mo atom was obtained from a Patterson synthesis, and the remainder of the molecule was located and refined by alternating difference Fourier maps and least-squares cycles. Anisotropic displacement parameters were assigned to all atoms other than carbon. Hydrogen atoms were not included in the model. The last cycle of refinement included the fit of 142 parameters to 1034 unique data with $F_o^2 > 3\sigma(F_o^2)$ and gave residuals of $R = 0.058$ and $R_w = 0.071$.

Table III. Positional Parameters and Their Estimated Standard Deviations for Compound **3**

atom	*x*	*y*	*z*	*B*, Å^2
Mo(1)	0.0717 (2)	0.0979 (1)	0.03561 (8)	3.63 (2)
S(1)	−0.0039 (6)	−0.0637 (3)	0.1015 (3)	4.8 (1)
P(1)	0.3824 (6)	0.4368 (4)	0.8367 (3)	4.9 (1)
F(1)	0.596 (1)	0.414 (1)	0.8397 (7)	11.1 (4)
F(2)	0.174 (2)	0.463 (1)	0.8305 (7)	11.7 (4)
F(3)	0.384 (2)	0.421 (1)	0.7425 (6)	10.6 (4)
F(4)	0.375 (2)	0.448 (1)	0.9305 (7)	13.3 (5)
F(5)	0.330 (2)	0.320 (1)	0.847 (1)	14.7 (6)
F(6)	0.428 (2)	0.560 (1)	0.826 (1)	13.3 (5)
O(1)	0.318 (1)	0.0951 (8)	0.0387 (6)	4.3 (2)
N(1)	0.072 (2)	0.2776 (9)	0.0057 (8)	4.1 (3)
N(2)	0.058 (2)	0.181 (1)	0.1579 (7)	4.2 (3)
N(3)	−0.237 (2)	0.155 (1)	0.0491 (7)	4.4 (3)
C(1)	−0.131 (3)	0.181 (2)	0.195 (1)	6.7 (4)*
C(2)	−0.287 (3)	0.183 (2)	0.138 (1)	6.8 (5)*
C(3)	−0.274 (3)	0.256 (1)	−0.002 (1)	6.9 (5)*
C(4)	−0.114 (2)	0.322 (1)	−0.019 (1)	6.4 (4)*
C(5)	0.156 (3)	0.341 (2)	0.074 (1)	7.5 (5)*
C(6)	0.137 (3)	0.293 (2)	0.155 (1)	7.4 (5)*

[a] Values marked with an asterisk indicate that the atoms were refined isotropically. Anisotropically refined atoms are given in the form of the isotropic equivalent thermal parameter defined as $^4/_3[a^2\beta_{11} + b^2\beta_{22} + c^2\beta_{33} + ab(\cos\gamma)\beta_{12} + ac(\cos\beta)\beta_{13} + bc(\cos\alpha)\beta_{23}]$.

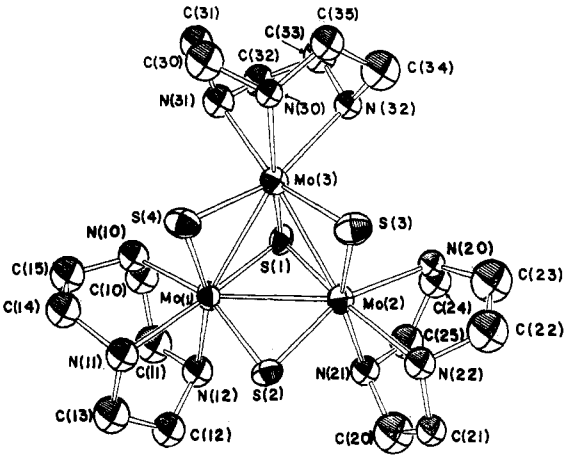

Figure 1. Perspective drawing of the cluster cation $[Mo_3S_4([9]aneN_3)_3]^{4+}$ (**2**). Atoms are represented by thermal ellipsoids at the 50% level.

Table I contains many data pertaining to data collection and refinement for both structures. The fractional coordinates for compounds **2** and **3** are listed in Tables II and III, respectively.

Results and Discussion

The molybdenum thiocubane aquo ion, in our experience, is a fairly robust species, and acidic solutions can be handled in air over extended time periods. We and others have observed that it is eventually converted into the trinuclear Mo_3S_4 aquo species, which we have characterized as the oxalate derivative.[8]

We now find that the [9]aneN$_3$ ligand enhances the lability of the cluster core as compared to the aquo species in that complete fragmentation occurs in acidic or neutral media within 1 day. It is interesting not only that the oxidative fragmentation results in well-defined products but also that both possible fragmentation modes, depending on the conditions, are realized, viz., $M_4 \rightarrow M_3 + M_1$ and $M_4 \rightarrow 2M_2$.

Under acidic conditions, the trinuclear compound, **2**, is isolated as the only colored product. It is a trinuclear cluster compound of Mo(IV) and belongs to the M_3X_{13} type of clusters.[9] A per-

(8) Cotton, F. A.; Dori, Z.; Llusar, R.; Schwotzer, W. *J. Am. Chem. Soc.* **1985**, *107*, 6734.
(9) Müller, A.; Jostes, R.; Cotton, F. A. *Angew Chem., Int. Ed. Engl.* **1980**, *19*, 875.

Table IV. Selected Bond Distances and Angles for Compound **2**[a]

(a) Bond Distances (Å)

Mo(1)–Mo(2)	2.766 (3)	Mo(2)–S(3)	2.291 (7)
Mo(1)–Mo(3)	2.779 (3)	Mo(2)–N(20)	2.29 (2)
Mo(1)–S(1)	2.354 (6)	Mo(2)–N(21)	2.29 (2)
Mo(1)–S(2)	2.278 (7)	Mo(2)–N(22)	2.21 (2)
Mo(1)–S(4)	2.271 (6)	Mo(3)–S(1)	2.372 (6)
Mo(1)–N(10)	2.22 (2)	Mo(3)–S(3)	2.282 (7)
Mo(1)–N(11)	2.23 (2)	Mo(3)–S(4)	2.265 (7)
Mo(1)–N(12)	2.36 (2)	Mo(3)–N(30)	2.25 (2)
Mo(2)–Mo(3)	2.775 (3)	Mo(3)–N(31)	2.30 (2)
Mo(2)–S(1)	2.356 (5)	Mo(3)–N(32)	2.31 (2)
Mo(2)–S(2)	2.282 (6)	Mo(3)–N(32)	2.31 (2)

(b) Bond Angles (deg)

Mo(2)–Mo(1)–Mo(3)	60.07 (7)	S(1)–Mo(2)–N(21)	89.6 (5)
Mo(2)–Mo(1)–S(1)	54.1 (1)	S(1)–Mo(2)–N(22)	160.6 (5)
Mo(2)–Mo(1)–S(2)	52.7 (2)	S(2)–Mo(2)–S(3)	96.2 (2)
Mo(2)–Mo(1)–S(4)	98.8 (2)	S(2)–Mo(2)–N(20)	158.7 (5)
Mo(2)–Mo(1)–N(10)	143.6 (5)	S(2)–Mo(2)–N(21)	92.3 (5)
Mo(2)–Mo(1)–N(11)	138.3 (5)	S(2)–Mo(2)–N(22)	87.1 (5)
Mo(2)–Mo(1)–N(12)	100.0 (5)	S(3)–Mo(2)–N(20)	94.3 (5)
Mo(3)–Mo(1)–S(1)	54.o (2)	S(3)–Mo(2)–N(21)	159.9 (5)
Mo(3)–Mo(1)–S(2)	98.1 (2)	S(3)–Mo(2)–N(22)	87.6 (5)
Mo(3)–Mo(1)–S(4)	52.1 (2)	N(20)–Mo(2)–N(21)	72.3 (6)
Mo(3)–Mo(1)–N(10)	102.2 (5)	N(20)–Mo(2)–N(22)	74.9 (6)
Mo(3)–Mo(1)–N(11)	138.2 (5)	N(21)–Mo(2)–N(22)	74.7 (7)
Mo(3)–Mo(1)–N(12)	144.2 (5)	Mo(1)–Mo(3)–Mo(2)	59.73 (7)
S(1)–Mo(1)–S(2)	105.4 (2)	Mo(1)–Mo(3)–S(1)	53.7 (2)
S(1)–Mo(1)–S(4)	104.7 (2)	Mo(1)–Mo(3)–S(3)	97.7 (2)
S(1)–Mo(1)–N(10)	89.5 (5)	Mo(1)–Mo(3)–S(4)	52.3 (2)
S(1)–Mo(1)–N(11)	163.1 (5)	Mo(1)–Mo(3)–N(30)	138.7 (4)
S(1)–Mo(1)–N(12)	90.0 (5)	Mo(1)–Mo(3)–N(31)	103.7 (5)
S(2)–Mo(1)–S(4)	98.2 (2)	Mo(1)–Mo(3)–N(32)	144.3 (4)
S(2)–Mo(1)–N(10)	159.4 (5)	Mo(2)–Mo(3)–S(1)	53.8 (1)
S(2)–Mo(1)–N(11)	85.5 (5)	Mo(2)–Mo(3)–S(3)	52.8 (2)
S(2)–Mo(1)–N(12)	89.8 (5)	Mo(2)–Mo(3)–S(4)	98.7 (2)
S(4)–Mo(1)–N(10)	91.4 (5)	Mo(2)–Mo(3)–N(30)	138.8 (4)
S(4)–Mo(1)–N(11)	86.1 (5)	Mo(2)–Mo(3)–N(31)	143.5 (5)
S(4)–Mo(1)–N(12)	160.7 (5)	Mo(2)–Mo(3)–N(32)	101.7 (4)
N(10)–Mo(1)–N(11)	77.0 (7)	S(1)–Mo(3)–S(3)	105.3 (2)
N(10)–Mo(1)–N(12)	75.9 (7)	S(1)–Mo(3)–S(4)	104.3 (2)
N(11)–Mo(1)–N(12)	77.0 (7)	S(1)–Mo(3)–N(30)	162.9 (5)
Mo(1)–Mo(2)–Mo(3)	60.21 (6)	S(1)–Mo(3)–N(31)	89.9 (5)
Mo(1)–Mo(2)–S(1)	54.0 (2)	S(1)–Mo(3)–N(32)	90.7 (5)
Mo(1)–Mo(2)–S(2)	52.6 (2)	S(3)–Mo(3)–S(4)	97.9 (2)
Mo(1)–Mo(2)–S(3)	97.9 (2)	S(3)–Mo(3)–N(30)	86.0 (5)
Mo(1)–Mo(2)–N(20)	143.5 (5)	S(3)–Mo(3)–N(31)	158.4 (5)
Mo(1)–Mo(2)–N(21)	101.8 (5)	S(3)–Mo(3)–N(32)	91.8 (5)
Mo(1)–Mo(2)–N(22)	139.6 (5)	S(4)–Mo(3)–N(30)	86.4 (5)
Mo(3)–Mo(2)–S(1)	54.3 (2)	S(4)–Mo(3)–N(31)	92.9 (5)
Mo(3)–Mo(2)–S(2)	98.1 (2)	S(4)–Mo(3)–N(32)	159.3 (5)
Mo(3)–Mo(2)–S(3)	52.5 (2)	Mo(1)–S(1)–Mo(2)	71.9 (2)
Mo(3)–Mo(2)–N(20)	103.0 (4)	Mo(1)–S(1)–Mo(3)	72.0 (2)
Mo(3)–Mo(2)–N(21)	143.9 (5)	Mo(2)–S(1)–Mo(3)	71.9 (2)
Mo(3)–Mo(2)–N(22)	140.0 (5)	Mo(1)–S(2)–Mo(2)	74.7 (2)
S(1)–Mo(2)–S(2)	105.2 (2)	Mo(2)–S(3)–Mo(3)	74.7 (2)
S(1)–Mo(2)–S(3)	105.6 (2)	Mo(1)–S(4)–Mo(3)	75.6 (2)
S(1)–Mo(2)–N(20)	89.6 (5)		

[a] Numbers in parentheses are estimated standard deviations in the least significant digits.

spective drawing of the cluster cation is presented in Figure 1. Table IV contains a list of important bond distances and angles. There are now several examples for this cluster type with W and Mo. A comparison of some of their geometrical properties (Table V) reveals some interesting trends. It is apparent that the M–M bond lengths, for the same number of cluster bonding electrons, are primarily affected by the nature of the capping and bridging ligands. For the M_3S_4 unit an average M–M bond length of 2.770 [6] Å is observed and there is no statistically significant dependence upon the nature of the terminal ligands, the metals (Mo or W), or the total charge of the cluster. Substitution of the bridging sulfido by oxo groups induces a shortening of the M–M bonds to 2.589 (?) and 2.612 [6] Å for Mo and W, respectively. The difference between the two metals is barefly significant ($\Delta/\sigma = 4$). For the M_3O_4 core we find average bond distances of 2.50

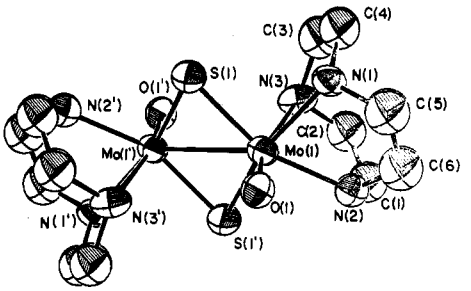

Figure 2. ORTEP view of the $[Mo_2S_2O_2([9]aneN_3)_2]^{2+}$ cation. The thermal ellipsoids enclose 50% of the electron density.

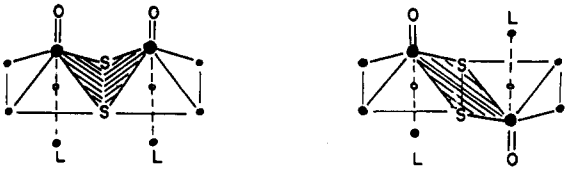

Figure 3. Schematic representation of edge-sharing bioctahedron with square-pyramidal distortion (syn and anti configuration).

[1] and 2.53 [1] Å for Mo and W, respectively. Again the difference is barely significant. However, for exact homologues the Mo–Mo distances are without exception shorter than the W–W distances. We have found before that in M–M bonded systems the core–core repulsion becomes important at internuclear distances shorter than ca. 2.50 Å while it plays a negligible role at larger M–M separations, and we refer to our earlier work for a more detailed discussion.[10] Two interesting compounds demonstrating the near additivity of substituent increment are Shibahara's $[Mo_3(\mu_3\text{-}S)(\mu\text{-}S)_2(\mu\text{-}O)(ida)_3]^{2-}$ and $[Mo_3(\mu_3\text{-}S)(\mu\text{-}S)(\mu\text{-}O)_2(NCS)_9]^{5-}$, in which the sulfido bridged edges are only slightly shorter than those of the Mo_3S_4 core while the oxo-bridged edges are very close to the bond length in the $Mo_3(\mu_3\text{-}S)(\mu\text{-}O)_3$ core.

The fragmentation pathway under neutral conditions is a different one, and a dinuclear disulfido-bridged oxomolybdenum(V) compound is isolated. A perspective drawing is presented in Figure 2. A list of important bond distances and angles is in Table VI. The compound has an edge-sharing bioctahedral configuration with an anti arrangement of the oxo ligands with respect to the $Mo(\mu\text{-}S)_2Mo$ plane. The Mo–Mo distance is 2.831 (2) Å and therefore consistent with the presence

(10) Cotton, F. A.; Dori, Z.; Marler, D. O.; Schwotzer, W. *Inorg. Chem.*, in press.
(11) Shibahara, T.; Miyake, H.; Kobayashi, K.; Kuroya, N. *Chem. Lett.* **1986**, 139.
(12) Shibahara, T.; Yamada, T.; Kyroya, H. *Inorg. Chim. Acta* **1986**, *113*, L19.
(13) Bino, A.; Cotton, F. A.; Dori, Z. *J. Am. Chem. Soc.* **1978**, *100*, 5252.
(14) Müller, A.; Ruck, A.; Dartmann, M.; Reinsch-Vogell, U. *Angew. Chem.* **1981**, *93*, 493.
(15) Bino, A.; Cotton, F. A.; Dori, Z. *J. Am. Chem. Soc.* **1979**, *101*, 3842.
(16) Shibahara, T.; Hattori, H.; Kuroya, H. J. *J. Am. Chem. Soc.* **1984**, *106*, 2710.
(17) Cotton, F. A.; Llusar, R.; Marler, D. O.; Schwotzer, W. *Inorg. Chem. Acta* **1985**, *102*, L25.
(18) Howlader, N. C.; Haight, G. P., Jr.; Hambley, T. W.; Lawrance, G. A.; Rahmoeller, K. M.; Snow, M. R. *Aust. J. Chem.* **1983**, *36*, 377.
(19) Halbert, T. R.; McGauley, K.; Pan, W.-H.; Gzeriozewicz, R. S.; Stiefeld, E. I. *J. Am. Chem. Soc.* **1984**, *106*, 1849.
(20) Segawa, M.; Sasaki, Y. *J. Am. Chem. Soc.* **1985**, *107*, 5565.
(21) Matles, R.; Mennemann, K. *Z. Anorg. Allg. Chem.* **1977**, *437*, 175.
(22) Chaudhun, P.; Wieghardt, K.; Gebert, W.; Jibril, J.; Huttner, G. *Z. Anorg. Allg. Chem.* **1985**, *521*, 23.
(23) Cotton, F. A.; Dori, Z.; Llusar, R.; Schwotzer, W. *Polyhedron* **1986**, *5*, 907.
(24) Shibahara, T.; Kohola, K.; Ohtsuji, A.; Yasuda, K.; Kuroya, H. *J. Am. Chem. Soc.* **1986**, *108*, 2757.
(25) Brown, D. H.; Jeffreys, J. A. D. *J. Chem. Soc., Dalton Trans.* **1973**, 732.
(26) Spivack, B.; Gaughan, A. P.; Dori, Z. *J. Am. Chem. Soc.* **1971**, *93*, 5266.
(27) Spivack, B.; Dori, Z. *J. Chem. Soc., Dalton Trans.* **1973**, 1173.
(28) Drew, M. G. B.; Kay, A. *J. Chem. Soc. A* **1971**, 1851.
(29) Stevenson, D. L.; Dahl, L. F. *J. Am. Chem. Soc.* **1967**, *89*, 3721.

Table V. Bond Lengths in Compounds Containing $Mo_3(\mu_3\text{-}X)(\mu\text{-}Y)_3$ Cores

cluster species	M–M, Å	M–μ_3-X, Å	M–μ-Y, Å	ref
$\{Mo_3(\mu_3\text{-}O)(\mu\text{-}O)_3(C_2O_4)_3(H_2O)_3\}^{2-}$	2.486 (1)	2.019 (6)	1.921 (7)	13
$\{Mo_3(\mu_3\text{-}O)(\mu\text{-}O)_3F_9\}^{5-}$	2.505 (?)			14
$\{Mo_3(\mu_3\text{-}O)(\mu\text{-}O)_3(EDTA)_{1.5}\}^{2-}$	2.505 (13)	2.04 (1)	1.92 (2)	15
$\{Mo_3(\mu_3\text{-}S)(\mu\text{-}O)_3(Hnta)_3\}^{2-}$	2.589	2.360	1.197	16
$\{Mo_3(\mu_3\text{-}S)(\mu\text{-}S)_2(\mu\text{-}O)(ida)_3\}^{2-}$	2.72 (1)[a]	2.35 (1)	2.31 (1)[a]	11
	2.612 (2)[b]		1.944 (8)[b]	
$\{Mo_3(\mu_3\text{-}S)(\mu\text{-}S)(\mu\text{-}O)_2(SCN)_9\}^{5-}$	2.715 (4)[a]	2.32 (1)	2.24 (1)[a]	12
	2.653 (3)[b]		1.94 (2)[b]	
$\{Mo_3(\mu_3\text{-}S)(\mu\text{-}S)_3[(nta)_3(H)_2]\}^{3-}$	2.769 (1)	2.344 (5)	2.298 (3)	17
$\{Mo_3(\mu_3\text{-}S)(\mu\text{-}S)_3(CN)_9\}^{5-}$	2.765 (7)	2.363 (4)	2.312 (5)	18
$\{Mo_3(\mu_3\text{-}S)(\mu\text{-}S)_3(SCH_2CH_2S)_3\}^{2-}$	2.78	2.35	2.30	19
$\{Mo_3(\mu_3\text{-}S)(\mu\text{-}S)_3(C_2O_4)_3(H_2O)_3\}^{2-}$	2.738 (5)	2.33 (1)	2.28 (1)	8
$\{Mo_3(\mu_3\text{-}S)(\mu\text{-}S)_3([9]aneN_3)_3\}^{4+}$	2.773 (1)	2.36 (1)	2.278 (9)	*c*
$\{W_3(\mu_3\text{-}O)(\mu\text{-}O)_3(SCN)_9\}^{5-}$	2.53 (1)			20
$\{W_3(\mu_3\text{-}O)(\mu\text{-}O)_3F_9\}^{5-}$	2.514 (2)	2.07 (1)	1.95 (3)	21
$\{W_3(\mu_3\text{-}O)(\mu\text{-}O)_3([9]aneN_3)_3\}^{4+}$	2.53 (1)	2.12 (1)	1.92 (1)	22
$\{W_3(\mu_3\text{-}S)(\mu\text{-}O)_3(SCN)_9\}^{5-}$	2.612 (6)	2.34 (2)	1.98 (2)	23
$\{W_3(\mu_3\text{-}S)(\mu\text{-}S)_3(SCN)_9\}^{5-}$	2.765 (3)	2.36 (2)	2.31 (1)	24

[a] S bridge. [b] O bridge. [c] This work.

Table VI. Selected Bond Distances and Angles for Compound **3**[a]

(a) Bond Distances (Å)

Mo(1)–Mo(1′)	2.831 (2)	Mo(1)–N(1)	2.238 (8)
Mo(1)–S(1)	2.503 (3)	Mo(1)–N(2)	2.231 (9)
Mo(1)–S(1′)	2.309 (3)	Mo(1)–N(3)	2.319 (9)
Mo(1)–O(1)	1.754 (7)		

(b) Bond Angles (deg)

Mo(1′)–Mo(1)–S(1)	52.22 (9)	S(1′)–Mo(1)–O(1)	102.6 (3)
Mo(1′)–Mo(1)–S(1′)	52.11 (8)	S(1′)–Mo(1)–N(1)	88.1 (3)
Mo(1′)–Mo(1)–O(1)	110.4 (2)	S(1′)–Mo(1)–N(2)	158.2 (2)
Mo(1′)–Mo(1)–N(1)	137.2 (2)	S(1′)–Mo(1)–N(3)	87.7 (3)
Mo(1′)–Mo(1)–N(2)	136.4 (2)	O(1)–Mo(1)–N(1)	91.3 (3)
Mo(1′)–Mo(1)–N(3)	87.3 (3)	O(1)–Mo(1)–N(2)	92.3 (3)
S(1)–Mo(1)–S(1′)	104.3 (1)	O(1)–Mo(1)–N(3)	162.2 (4)
S(1)–Mo(1)–O(1)	102.2 (3)	N(1)–Mo(1)–N(2)	75.6 (3)
S(1)–Mo(1)–N(1)	159.0 (3)	N(1)–Mo(1)–N(3)	74.4 (3)
S(1)–Mo(1)–N(2)	87.6 (3)	N(2)–Mo(1)–N(3)	74.2 (3)
S(1)–Mo(1)–N(3)	89.0 (3)	Mo(1)–S(1)–Mo(1′)	75.7 (1)

[a] Numbers in parentheses are estimated standard deviations in the least significant digits.

Table VII. Structural Parameters of Complexes Containing the $Mo_2O_2S_2^{2+}$ Group

compd	Mo–Mo, Å	Mo–S, Å	dihedral angle, deg	ref
$Na_2Mo_2O_2S_2(cys)_2$	2.820 (3)	2.330 (9)	156	25
$Na_2Mo_2O_2S_2(his)_2\cdot 5H_2O$	2.82 (1)	2.32 (2)	160.9 (9)	26
$Cs_2Mo_2O_2S_2(edta)\cdot 2H_2O$	2.779 (1)	2.289 (1)	152.3 (2)	27
$Mo_2O_2S_2(cys\text{-}Me\text{-}ester)_2$	2.804 (4)	2.31 (1)	149.1	28
$\{Mo_2O_2S_2([9]aneN_3)_2\}(PF_6)_2$	2.831 (2)	2.307 (3)	180	*a*
$Mo_2O_2S_2(C_5H_5)_2$	2.894 (5)	2.317 (3)	180	29

[a] This work.

of a M–M single bond. Important geometrical properties can be compared with those of structurally related compounds with the data in Table VII. It is apparent that the Mo–Mo distances in compounds with syn configuration are systematically shorter than in those with anti configuration. Furthermore, the anti arrangement entails coplanarity of the metal centers and the bridging sulfur atoms whereas there is a butterfly-shaped envelope for the same substructure in all the syn compounds. This can conveniently been rationalized by geometrical considerations involving edge-sharing bioctahedra with a distortion toward square pyramids (Figure 3). The distortion arises from a displacement of the metal atom from the equatorial plane toward the oxo ligand with a concomitant lengthening of the M–L bond in trans position to the oxo group. Combining two such distorted octahedra in a syn configuration leads to the observed butterfly envelope. The M–M distance, in the idealized case, is insensitive to the degree of distortion, which will depend on the donor properties of the trans ligand. Alternatively, if the octahedra are fused in a trans fashion, the resulting arrangement is strictly planar. Furthermore, the M–M distance will strongly depend upon the degree of distorsion and generally increase as weaker donor ligands occupy the trans position.

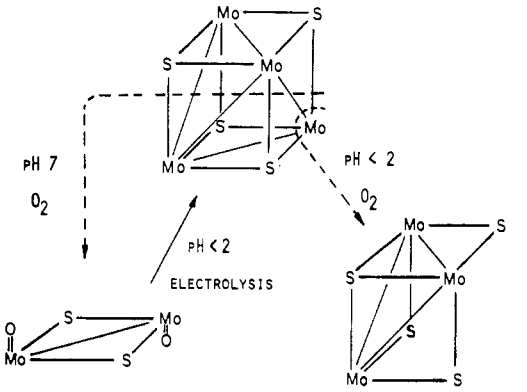

Figure 4. Fragmentation pathways for the molybdenum thiocubane.

Finally, both compounds are the products of oxidative fragmentation with air oxygen being the most likely oxidant. The formal fragmentation pathways are outlined in Figure 4. The product from acidic solution, trinuclear cluster **2**, has the structural features of an incomplete cube. The fate of the extruded Mo vertex is unknown. We have observed an analogous fragmentation before with acidic solutions of the Mo_4S_4 aquo ion and during attempts to derivatize the latter with the oxalate ligand.[8] The second pathway, which has not been reported before, involves not only oxidation but also hydrolysis. It is therefore not surprising that it occurs under neutral conditions, which are known to foster the formation of oxo species for various oxidation states of Mo, most prominently Mo(V) and Mo(VI). Incidentally, this fragmentation mode corresponds to the reverse of the reaction in Sykes' synthesis of the Mo_4S_4 aquo ion from dinuclear Mo(V) precursors.[3]

Acknowledgment. We are grateful to Professor Karl Wieghardt for providing a sample of 1,4,7-triazacyclononane trihydrobromide and to the National Science Foundation for financial support.

Registry No. **1**, 103731-75-5; **2**, 103731-78-8; **3**, 103731-80-2.

Supplementary Material Available: Tables of bond distances and angles and anisotropic thermal parameters (7 pages); tables of observed and calculated structure factors (19 pages). Ordering information is given on any current masthead page.